

The Effects of Weak Spatiotemporal Noise on a Bistable One-Dimensional System

Robert S. Maier^(a,b) and D. L. Stein^(b,a)
Depts. of ^(a)Mathematics and ^(b)Physics
University of Arizona
Tucson, AZ 85721, USA

Abstract

We treat analytically a model that captures several features of the phenomenon of spatially inhomogeneous reversal of an order parameter. The model is a classical Ginzburg–Landau field theory restricted to a bounded one-dimensional spatial domain, perturbed by weak spatiotemporal noise having a flat power spectrum in time and space. Our analysis extends the Kramers theory of noise-induced transitions to the case when the system acted on by the noise has nonzero spatial extent, and the noise itself is spatially dependent. By extending the Langer–Coleman theory of the noise-induced decay of a metastable state, we determine the dependence of the activation barrier and the Kramers reversal rate prefactor on the size of the spatial domain. As this is increased from zero and passes through a certain critical value, a transition between activation regimes occurs, at which the rate prefactor diverges. Beyond the transition, reversal preferentially takes place in a spatially inhomogeneous rather than in a homogeneous way. Transitions of this sort were not discovered by Langer or Coleman, since they treated only the infinite-volume limit. Our analysis uses higher transcendental functions to handle the case of finite volume. Similar transitions between activation regimes should occur in other models of metastable systems with nonzero spatial extent, perturbed by weak noise, as the size of the spatial domain is varied.

1 Introduction

The phenomenon of noise-induced escape from a metastable state, and the related phenomenon of noise-induced transitions between the stable states of a bistable system, occur in many places in the sciences and engineering [1]. Our focus in this paper is the case when the system on which the noise acts has nontrivial spatial extent, and the noise is not spatially uniform, but has significant spatial dependence. This case arises in numerous physical contexts, in both equilibrium and non-equilibrium systems. Examples of noise-induced transitions in spatially extended systems include pattern formation in convective and electroconvective systems far from equilibrium [2, 3], thermally activated magnetization reversal in nanomagnets [4, 5], vortex creep in superconductors [6], the growth of instabilities in metallic nanowires [7], and many others.

Possibly the simplest mathematical model of a spatially extended system undergoing a noise-induced transition is a Ginzburg–Landau scalar field theory perturbed by weak spatiotemporal noise. Even here, the mathematical complexity of the problem has restricted most treatments to the case of one spatial dimension. The phenomenon of classical nucleation on a line was treated by Langer [8] in a seminal paper, and a closely related quantum phenomenon was treated by Callan and Coleman [9]. In the limit as the size of the one-dimensional spatial domain tends to infinity, they were able to compute (respectively) the nucleation rate per unit length, and what amounts to a tunnelling rate per unit length. Their work has been widely applied and cited.

However, many practical applications require an understanding of the phenomenon of noise-induced nucleation in systems with a spatial extent that is both nonzero and non-infinite, and the extent to which the nucleation rate per unit length depends on system size. Noise-induced transitions between the two stable states of a bistable nonlinear field theory, in a finite-volume domain, have been investigated by several authors [10, 11, 12]. The difference between finite and infinite systems is not merely quantitative. Recently, the authors [13] uncovered an unusual effect, akin to a phase transition, that occurs in an overdamped classical Ginzburg–Landau field theory with a bistable ϕ^4 potential, as the length L of its one-dimensional spatial domain is varied. A similar phenomenon had previously been seen in a quantum context [14, 15]. The lowest-energy ‘saddle’ between the two stable configurations, through which noise-activated transitions preferentially occur (especially when the noise strength is low) may bifurcate. Below a critical length L_c , this transition state is a spatially constant field configuration, but at $L = L_c$ it bifurcates into a spatially varying pair of configurations, degenerate in energy. Subsequent work [16] shows that a similar bifurcation occurs in a Ginzburg–Landau model with an asymmetric potential, in which the two new spatially varying transition states are not degenerate; so one or the other is preferred. The ‘phase transition’ at a critical length L_c is therefore reasonably robust.

So at a critical system size, there may occur a major change in the phenomenology of noise-induced transitions between the stable states of a Ginzburg–Landau field theory, which proceed via nucleation. Associated with the bifurcation of the transition state is a bifurcation of the MPEP (most probable escape path, i.e., transition path in configuration space) extending uphill from each stable state to the transition state. The bifurcation is driven by this preferred nucleation pathway becoming unstable in the transverse direction. As one would expect, the transition rate is strongly affected by the bifurcation. Formally, the prefactor in the Kramers (weak-noise) nucleation rate *diverges* at $L = L_c$. This signals that precisely at $L = L_c$, the phenomenon of transition between the two stable states becomes non-Arrhenius: the rate at which it occurs falls off in the limit of weak noise not like an exponential (with a constant prefactor), but rather like an exponential with a power-law prefactor.

Our paper Ref. [13] computed the Kramers prefactor as a function of L , through the bifurcation, by using elliptic functions. The use of higher transcendental functions made it possible to treat the case $L < \infty$, i.e., to go beyond the analyses of Langer, and Callan and Coleman. However, we considered in detail only the case when Dirichlet conditions are imposed on the Ginzburg–Landau field at the endpoints of the spatial domain. How sensitive is the occurrence of a phase transition at some $L = L_c$ to the boundary conditions employed? We examine this question here, by extending our qualitative results and nucleation rate computations to the cases of Neumann, periodic, and

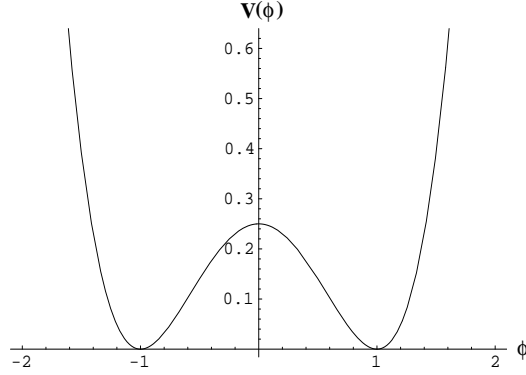


Figure 1: Bistable potential for the order parameter ϕ given by Eq. 1.

antiperiodic boundary conditions. We shall show that the phase transition is robust to changes in boundary condition, but that unsurprisingly, there are quantitative differences among the various cases. Examination of these differences will permit us to present our methods in more detail, and provide further insights into the behavior of noise-activated transitions in spatially extended systems.

2 Model and Phenomenology

Consider an order parameter ϕ governed by a bistable quartic potential energy function that may be written in dimensionless units as

$$V(\phi) = (\phi^2 - 1)^2/4. \quad (1)$$

This potential is shown in Fig. 1. The stable states $\phi = \pm 1$ are degenerate, with zero energy. If ϕ evolves in a deterministic, overdamped way, it will satisfy the equation $\dot{\phi} = -V'(\phi)$. If it is perturbed by additive white noise, it will satisfy, instead, $\dot{\phi} = -V'(\phi) + \epsilon^{1/2}\xi(t)$. Here ξ is unit-strength temporal white noise, satisfying $\langle \xi(t_1)\xi(t_2) \rangle = \delta(t_1 - t_2)$, and ϵ is the noise strength. In a thermal context, $\epsilon \propto kT$.

We shall treat here the case when ϕ is actually a classical field on a one-dimensional spatial domain: in dimensionless units, the interval $[0, L]$. The simplest extension of the overdamped stochastic evolution equation to incorporate spatial effects is the stochastic Ginzburg–Landau equation

$$\begin{aligned} \dot{\phi} &= \phi'' - V'(\phi) + \epsilon^{1/2}\xi(x, t) \\ &= \phi'' + \phi - \phi^3 + \epsilon^{1/2}\xi(x, t), \end{aligned} \quad (2)$$

where $\xi(x, t)$ is unit-strength spatiotemporal white noise, which is defined to satisfy $\langle \xi(x_1, t_1)\xi(x_2, t_2) \rangle = \delta(x_1 - x_2)\delta(t_1 - t_2)$. Zero-noise dynamics will be ‘gradient’, i.e., conservative. That is, if $\epsilon = 0$, then

$$\dot{\phi} = -\delta\mathcal{H}/\delta\phi, \quad (3)$$

where

$$\mathcal{H}[\phi] \equiv \int_0^L \left[\frac{1}{2}(\phi')^2 + V(\phi) \right] dx \quad (4)$$

is the energy functional. So the statistical properties of the stochastically evolving field ϕ are described by equilibrium statistical mechanics. However, just as in the model without spatial extent, nonzero noise can induce transitions between the stable states, which naively are the two field configurations $\phi \equiv \pm 1$. This will typically occur via nucleation. A droplet of one stable configuration will form in a background of the other, and will ‘nucleate’: under the driving influence of the noise, it will spread to fill the entire spatial domain. Of course, it is more likely for a small droplet to shrink and vanish, especially when the noise is weak.

In the infinite-dimensional configuration space, an MPEP goes ‘uphill’ from each stable field configuration, leading to a preferred transition configuration (saddle) that lies between them. Each of these MPEPs is a nucleation pathway, i.e., a path of least resistance. By time-reversal invariance, each MPEP is a time-reversed zero-noise ‘downhill’ trajectory. If the noise is weak, the order parameter is expected to flip between the two stable configurations in a Markov way, with the expected waiting time in the basin of attraction of each being an exponential random variable, as is typical of slow rate processes. The activation rate (the reciprocal of the mean time between flips) will be given in the $\epsilon \rightarrow 0$ limit by the Kramers formula

$$\Gamma \sim \Gamma_0 \exp(-\Delta W/\epsilon). \quad (5)$$

Here ΔW is the activation barrier, which quantifies the extent to which the preferred transition configuration between the two stable configurations is energetically disfavored, and Γ_0 is the rate prefactor. Due to the normalization convention implicit in (2), $\Delta W = 2\Delta E$, where ΔE is the energy of the transition state minus the energy of either stable state. Here energy is computed from the functional $\mathcal{H}[\cdot]$ of (4). The factor of 2 arises from our decision to multiply unit-strength spatiotemporal noise by $\epsilon^{1/2}$ rather than by $\sqrt{2\epsilon}$.

The calculation of ΔW and Γ_0 will make up the technical component of this paper. Since we are using dimensionless units, they will depend only on the length L and the choice of boundary conditions at the endpoints $x = 0$ and $x = L$. The boundary conditions affect the way in which order parameter reversal occurs, since they may force nucleation to begin, preferentially, at the endpoints. It should also be noted that for some choices of boundary conditions, the stable states may only be approximations to the uniform $\phi \equiv \pm 1$ configurations.

3 The Stable and Transition States

We begin by examining the stationary solutions of the noiseless ($\epsilon = 0$) evolution equation. These will depend on the interval length L and the boundary conditions. The four boundary conditions we consider are periodic (P), antiperiodic (AP), Dirichlet (D), and Neumann (N). All four, applied to the stochastic Ginzburg–Landau equation, have potential applicability in physical modelling. For example, in modelling thermally activated magnetization reversal in a finite-length ferromagnetic nanowire, Neumann boundary conditions are appropriate [17]. The original treatments of Langer and Callan–Coleman used periodic boundary conditions; and so forth.

Periodic.—The conditions are $\phi(0) = \phi(L)$, $\phi'(0) = \phi'(L)$. There are three constant time-independent solutions: $\phi \equiv \pm 1$, each with energy 0; and $\phi \equiv 0$, with energy $1/4$. It is easy to see that $\phi \equiv \pm 1$ are stable for any L , and $\phi \equiv 0$ is always unstable. However, nonconstant solutions may also exist for a range of L . These will be considered below.

Antiperiodic.—The conditions are $\phi(0) = -\phi(L)$, $\phi'(0) = -\phi'(L)$. The only constant time-independent solution is $\phi \equiv 0$.

Dirichlet.—Only the conditions $\phi(0) = \phi(L) = 0$ will be considered here. Many other Dirichlet boundary conditions could be examined, but this case is particularly interesting because when L is sufficiently large, it has two nonconstant stationary solutions, which permits the possibility of a noise-induced transition. This is the case that was treated in Ref. [13].

Neumann.—Though there are many possibilities, we consider here only the conditions $\phi'(0) = \phi'(L) = 0$. The constant solutions here are the same as for periodic boundary conditions, but it will be seen that there are important differences between the two cases.

What *nonconstant* time-independent solutions exist when $\epsilon = 0$? By (2), any stationary solution satisfies

$$\phi'' = -\phi + \phi^3, \quad (6)$$

subject to the given boundary condition. That is, $\dot{\phi} = -\delta\mathcal{H}/\delta\phi = 0$. The linearized noiseless dynamics in the vicinity of such a state are specified by the Hessian operator $\delta^2\mathcal{H}/\delta\phi^2$. Stationary configurations for which this operator has all positive eigenvalues are stable; those with a single negative eigenvalue are possible transition states. For the latter, the eigenvector corresponding to the negative eigenvalue is the direction along which the MPEP approaches, in the infinite-dimensional configuration space. Nonconstant transition states are often called *instanton states*, in a nomenclature derived from Callan and Coleman [9]. In ϕ^4 and other theories, the term ‘instanton’ usually refers to a kink-like field configuration $\phi = \phi(x)$ asymptotic to $\phi = \pm 1$ as $x \rightarrow \pm\infty$, with a single node [18].

To satisfy the specified boundary conditions on $[0, L]$, a rather different sort of instanton state must be used. It is easy to check that the so-called *periodic instanton* $\phi = \phi_{\text{inst},m}(x)$ is a time-independent solution of (2) for any m in the range $0 < m \leq 1$. Here (cf. Ref. [19]),

$$\phi_{\text{inst},m}(x) \equiv \sqrt{\frac{2m}{m+1}} \text{sn}(x/\sqrt{m+1} \mid m), \quad (7)$$

where $\text{sn}(\cdot \mid m)$ is the Jacobi elliptic sn function with parameter m . Its quarter-period is given by $\mathbf{K}(m)$, the complete elliptic integral of the first kind [20], which is a monotonically increasing function of m . It can be viewed as an infinite alternating sequence of kinks and anti-kinks, spaced a distance $2\mathbf{K}(m)$ apart. As $m \rightarrow 0^+$, $\mathbf{K}(m)$ decreases to $\pi/2$, and $\text{sn}(\cdot \mid m)$ degenerates to $\sin(\cdot)$. As $m \rightarrow 1^-$, the quarter-period increases to infinity (with a logarithmic divergence), and $\text{sn}(\cdot \mid m)$ degenerates to the nonperiodic function $\tanh(\cdot)$, which is the canonical single-kink sigmoidal function. It is no accident that the hyperbolic tangent function appeared in the Langer and Callan–Coleman analyses in connection with the limiting ($L \rightarrow \infty$) shape of a critical droplet. For a careful recapitulation, see Ref. [21].

In the present context, the value of m in (7) is determined by the interval length L and the boundary conditions, as follows.

Periodic.—As stated earlier, the uniform configurations $\phi \equiv \pm 1$ are the stable states for all L . If the nonuniform solution (7) is to satisfy the boundary conditions, then L must be an integer multiple of a full period. It is obvious that larger integers correspond to higher energies (and therefore activation barriers); so the physically relevant nonuniform transition state is $\phi = \phi_{\text{inst},m_{u,P}}(x)$, where $m_{u,P}$ is determined implicitly by

$$4\sqrt{m_{u,P} + 1} \mathbf{K}(m_{u,P}) = L. \quad (8)$$

The subscript u denotes an unstable (i.e., transition) state and P denotes periodic boundary conditions. Similarly, s will denote a stable state, and the other boundary conditions will be correspondingly abbreviated.

This nonuniform stationary state is not present for all L : there is a minimum value of L , corresponding to $m = 0$, below which no solution of the form $\phi = \phi_{\text{inst},m_{u,P}}(x)$ can be constructed. That is, because $\mathbf{K}(0) = \pi/2$, the nonuniform transition state cannot occur below $L = 2\pi$. Below this value, the only possible transition state is the uniform state $\phi \equiv 0$. This solution remains an unstable stationary state for $L > 2\pi$, but with higher energy than that of the instanton state.

These considerations suggest the following qualitative picture of the periodic-b.c. case, to be justified subsequently by an energy and eigenvalue analysis. Suppose the system is in one of the two stable states $\phi \equiv \pm 1$. How does a transition induced by (weak) noise to the other state proceed? If $L < 2\pi$, the system preferentially ‘climbs uphill’ to the $\phi \equiv 0$ state, after which it ‘rolls downhill’ to the other stable state. So reversal of the order parameter preferentially takes place in a spatially homogeneous way. If $L > 2\pi$, however, there is another saddle, lower in energy than the instanton state and therefore a much more probable intermediate state when the noise strength is small. This is the instanton configuration $\phi = \phi_{\text{inst},m_{u,P}}(x)$, which is positive on half the interval and negative on the other half. This configuration can be thought of as a ‘droplet pair’, in which half the spatial domain is occupied, to a first approximation, by each of the two stable values of ϕ . Equivalently, it can be viewed as a configuration with a kink and an anti-kink, or two Bloch walls (if one is modelling a magnetic system). A transition occurs in the following way: a small droplet of the reversed value for the order parameter is formed, and under the driving influence of the noise, it grows to occupy half the interval. At that point, the saddle has been reached, and the droplet continues growing of its own accord until it fills the remainder of the interval, i.e., ‘rolls downhill’. Both halves of the transition can be interpreted in terms of kink motion: the uphill half being noise-driven, and the downhill half being deterministic.

Actually, there is a complication here: due to the translation symmetry that accompanies periodic boundary conditions, the transition state is necessarily infinitely degenerate. That is, $\phi = \phi_{\text{inst},m_{u,P}}(x - x_0)$, for any x_0 , will serve as a transition state. In physical language, the kink–anti-kink pair, i.e., the droplet, may form anywhere along the interval, leading (in the $L \rightarrow \infty$ limit) to a transition rate *per unit length*. We treat this matter elsewhere [22] (see also Ref. [16]).

Antiperiodic.—In this case there is a nonuniform stable state of the form $\phi = \phi_{\text{inst},m_{s,AP}}$, with $m_{s,AP}$ defined implicitly by

$$2\sqrt{m_{s,AP} + 1} \mathbf{K}(m_{s,AP}) = L, \quad (9)$$

However, this equation has no solution when $L < \pi$; in this range there is a single stable state given by $\phi \equiv 0$, and no possibility of an accompanying transition. The $\phi \equiv 0$ solution becomes

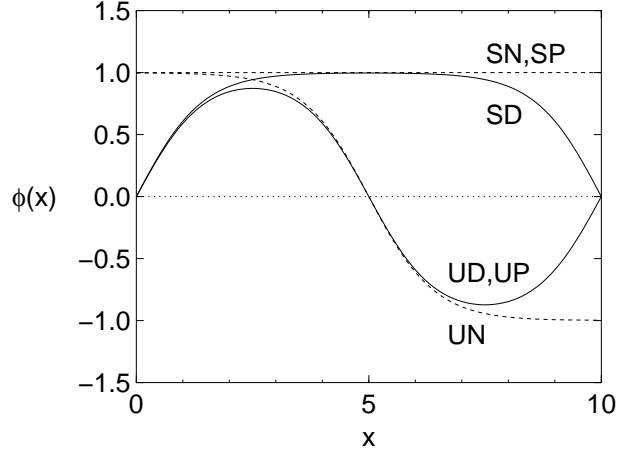


Figure 2: The stable states (S) and transition states (U), for periodic (P), Dirichlet (D), and Neumann (N) boundary conditions, when $L = 10$. Each nonzero state has a degenerate counterpart obtained by $\phi \mapsto -\phi$, and UP may be shifted arbitrarily, so it is infinitely degenerate. (From Ref. [13].)

unstable when $L > \pi$, and in fact is the transition state for $\pi < L < 3\pi$. For larger L this transition state undergoes a pitchfork bifurcation into a pair of instanton states with *three* half-wavelengths in the interval $[0, L]$. That is,

$$6\sqrt{m_{u,AP} + 1} \mathbf{K}(m_{u,AP}) = L. \quad (10)$$

As in the periodic case, this nonuniform transition state is infinitely degenerate; and the nonuniform stable state is too.

Dirichlet.—This case was examined in detail in Ref. [13]. If $L \leq \pi$, the model is monostable with the configuration $\phi \equiv 0$ as the only stable state. When L increases through π , this state undergoes a pitchfork bifurcation into a pair of stable configurations with

$$2\sqrt{m_{s,D} + 1} \mathbf{K}(m_{s,D}) = L. \quad (11)$$

In the range $0 \leq L \leq 2\pi$, the $\phi \equiv 0$ configuration is the transition state. It undergoes a pitchfork bifurcation at $L = 2\pi$; for larger values of L the parameter m of the transition state is determined by

$$4\sqrt{m_{u,D} + 1} \mathbf{K}(m_{u,D}) = L. \quad (12)$$

Note that the Dirichlet condition (and the Neumann condition, to be discussed below), pin the nonuniform stationary states at the boundaries, so that there is no issue of infinite degeneracy arising from translation symmetry to complicate the analysis. In physical terms, each of the two preferred nucleation pathways begins with the formation of a droplet at either end of the interval. As $L \rightarrow \infty$, it is not natural to speak of a transition rate per unit length.

Neumann.—Here the stable states are the uniform states $\phi \equiv \pm 1$. Also, if $L \leq \pi$ the transition state is the uniform configuration $\phi \equiv 0$. When L is increased through π , the transition state bifurcates into a pair of instanton states with the first argument of the Jacobi elliptic sn function in (7) shifted by $\mathbf{K}(m)$, a quarter wavelength (equivalent here to $L/2$). That is, the transition state is given by

$$\sqrt{\frac{2m}{m+1}} \operatorname{sn}(x/\sqrt{m+1} + \mathbf{K}(m) | m), \quad (13)$$

with $m = m_{u,N}$, a quantity determined implicitly by

$$2\sqrt{m_{u,N} + 1} \mathbf{K}(m_{u,N}) = L. \quad (14)$$

So $m_{u,N} = m_{s,D}$. In fact, up to a uniform shift, the Neumann-case transition state is the same as the Dirichlet-case stable state.

The results so far are summarized in Fig. 2, which depicts the stable and transition states for the cases of periodic, Dirichlet, and Neumann boundary conditions (the antiperiodic case is excluded for figure clarity). Each plotted nonconstant curve consists of an integer number of kinks or anti-kinks; or more accurately, an even number of half-kinks or half-anti-kinks.

4 The Activation Barrier

As mentioned in Sec. 2, the exponential falloff of the transition rate in the limit of weak noise, i.e., its Arrhenius behavior, is determined by the activation barrier ΔW between the two stable states. We noted that $\Delta W = 2\Delta E = 2(\mathcal{H}[\phi_u] - \mathcal{H}[\phi_s])$, with the energy functional $\mathcal{H}[\phi]$ given by (4). We shall call ΔE the ‘activation energy’. The calculation of $\mathcal{H}[\phi_s]$ and $\mathcal{H}[\phi_u]$, the stable and transition state energies, is trivial in the case of uniform states, and reasonably straightforward in the case of nonuniform (instanton) states, if standard elliptic function formulas [20] are used. The results are as follows.

Periodic.—If $L < L_c^P = 2\pi$, then trivially, $\Delta E = L/4$. If $L > L_c^P$, then

$$\Delta E = \frac{1}{3\sqrt{1+m_{u,P}}} \left[8\mathbf{E}(m_{u,P}) - \frac{(1-m_{u,P})(3m_{u,P}+5)}{(1+m_{u,P})} \mathbf{K}(m_{u,P}) \right], \quad (15)$$

where $\mathbf{E}(m)$ is the complete elliptic integral of the second kind [20]. Note that as $m_{u,P} \rightarrow 0^+$, i.e., $L \rightarrow (2\pi)^+$, the two regions connect in a smooth manner: ΔE is differentiable with respect to L at $L = 2\pi$, though not twice differentiable (the same relatively smooth join will obtain in all succeeding cases).

As $m_{u,P} \rightarrow 1^-$ (i.e., $L \rightarrow \infty$), $\Delta E \rightarrow 4\sqrt{2}/3$. This is a familiar quantity: it is twice the energy of a ϕ^4 kink [18]. The factor of 2 is due to the transition state configuration ϕ_u , the stationary periodic instanton solution, having two nodes, i.e., two swings between $\phi = \pm 1$ as x varies from 0 to L . In field theory language, it comprises a kink and an anti-kink.

Antiperiodic.—In the range $\pi < L \leq 3\pi$,

$$\Delta E = \frac{2}{3(1+m_{s,AP})^{3/2}} \left[(m_{s,AP} + 2)\mathbf{K}(m_{s,AP}) - 2(m_{s,AP} + 1)\mathbf{E}(m_{s,AP}) \right]. \quad (16)$$

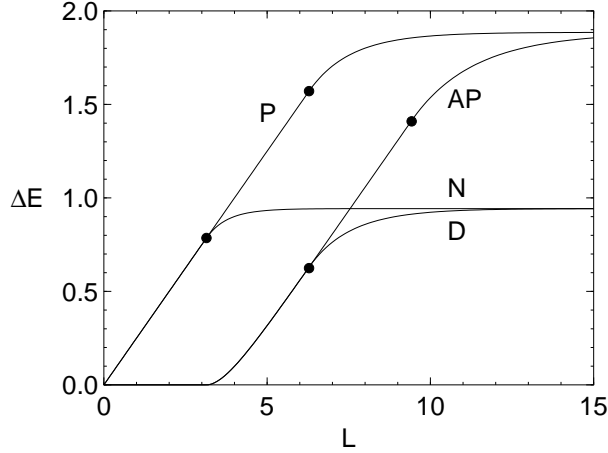


Figure 3: The activation energy ΔE as a function of the interval length L , for periodic (P), antiperiodic (AP), Dirichlet (D), and Neumann (N) boundary conditions. Bullets indicate critical interval lengths, at which bifurcations take place ($L_c^N = \pi$; $L_c^D = L_c^P = 2\pi$; and $L_c^{AP} = 3\pi$).

If $L > L_c^{AP} = 3\pi$, then

$$\Delta E = \frac{4}{3} \left[\frac{3}{\sqrt{1 + (m_{u,AP})}} \mathbf{E}(m_{u,AP}) - \frac{1}{\sqrt{1 + (m_{s,AP})}} \mathbf{E}(m_{s,AP}) \right] - \frac{1}{6} \left[\frac{3(1 - m_{u,AP})}{(1 + m_{u,AP})^{3/2}} (3m_{u,AP} + 5) \mathbf{K}(m_{u,AP}) - \frac{1 - m_{s,AP}}{(1 + m_{s,AP})^{3/2}} (3m_{s,AP} + 5) \mathbf{K}(m_{s,AP}) \right]. \quad (17)$$

It is noteworthy that as $m_{u,AP} \rightarrow 1^-$, $\Delta E \rightarrow 4\sqrt{2}/3$, just as in the periodic case. In the periodic case, the transition state has two nodes while the stable state has zero nodes; in the antiperiodic case, the transition state has three nodes while the stable state has one node. It is therefore not surprising that in both cases, the energy difference converges to twice the energy of a ϕ^4 kink as $L \rightarrow \infty$. Note that for any finite L , the relevant m values differ between the periodic and antiperiodic cases, but all approach unity from below as $L \rightarrow \infty$.

Dirichlet.—If $L \leq L_c^D = 2\pi$, then

$$\Delta E = \frac{2}{3(1 + m_{s,D})^{3/2}} \left[(m_{s,D} + 2) \mathbf{K}(m_{s,D}) - 2(m_{s,D} + 1) \mathbf{E}(m_{s,D}) \right], \quad (18)$$

which has the same form as (16). If $L > L_c^D$, then

$$\Delta E = \frac{4}{3} \left[\frac{2}{\sqrt{1 + (m_{u,D})}} \mathbf{E}(m_{u,D}) - \frac{1}{\sqrt{1 + (m_{s,D})}} \mathbf{E}(m_{s,D}) \right] - \frac{1}{6} \left[\frac{2(1 - m_{u,D})}{(1 + m_{u,D})^{3/2}} (3m_{u,D} + 5) \mathbf{K}(m_{u,D}) - \frac{1 - m_{s,D}}{(1 + m_{s,D})^{3/2}} (3m_{s,D} + 5) \mathbf{K}(m_{s,D}) \right]. \quad (19)$$

In the $L \rightarrow \infty$ limit, $\Delta E \rightarrow 2\sqrt{2}/3$, which is half the value for the periodic and antiperiodic cases. This is because the transition state now has only one more node than the stable state, rather than two. The same is true of the Neumann case. Hence these two latter cases will have the same activation energy in the $L \rightarrow \infty$ limit, just as the periodic and antiperiodic values for ΔE converge in this limit; and it will be the energy of a single ϕ^4 kink.

Neumann.—If $L \leq L_c^N = \pi$, then $\Delta E = L/4$; both the stable and transition states are the same here as in the low- L regime of the periodic case. If $L > L_c^N$, then

$$\Delta E = \frac{1}{3(1 + m_{u,N})^{3/2}} \left[4(1 + m_{u,N})\mathbf{E}(m_{u,N}) - \frac{1}{2}(1 - m_{u,N})(3m_{u,N} + 5)\mathbf{K}(m_{u,P}) \right], \quad (20)$$

As noted, the activation energy in the $L \rightarrow \infty$ limit equals $2\sqrt{2}/3$, as in the Dirichlet case.

The above formulas for the activation energy ΔE as a function of L are plotted in Fig. 3. The bifurcations at $L = \pi$, $L = 2\pi$, and $L = 3\pi$ are apparent, as is the differentiability (and lack of twice differentiability) through each bifurcation.

5 The Transition Rate Prefactor

As explained, the activation energy is (up to a factor of 2) equal to the activation barrier ΔW in the Kramers transition rate formula $\Gamma \sim \Gamma_0 \exp(-\Delta W/\epsilon)$, $\epsilon \rightarrow 0$. Calculation of the prefactor Γ_0 is a much more involved matter. In general, it requires an analysis of the *transverse fluctuations* about the MPEPs that go uphill to the transition state. In any ‘zero-dimensional’ (i.e., non-spatially-extended) equilibrium system, in which the noise-perturbed evolution equation is a stochastic *ordinary* differential equation, it is known that it suffices to compute the eigenvalues of the linearized dynamics at the endpoints of each MPEP, i.e., in the vicinity of the stable states and transition state [23]. For example, a system with a two-dimensional order parameter ϕ satisfying the overdamped evolution equation $\dot{\phi} = \mathbf{u}(\phi) + \epsilon^{1/2}\xi$, where $\mathbf{u} = \mathbf{u}(\phi)$ is a drift field that is the negative gradient of a potential, will have the Kramers escape rate

$$\Gamma \sim \frac{1}{2\pi} \sqrt{|\lambda_{\parallel}(U)| \lambda_{\parallel}(S)} \sqrt{\frac{\lambda_{\perp}(S)}{\lambda_{\perp}(U)}} \exp(-\Delta W/\epsilon), \quad \epsilon \rightarrow 0. \quad (21)$$

Here S denotes the stable fixed point of \mathbf{u} and U the saddle point over which escape from the basin of attraction of S preferentially occurs. $\lambda_{\parallel}(S) = -\partial u_{S,1}/\partial \phi_{S,1}$ is the eigenvalue of the linearized negative drift field at S whose corresponding eigenvector points along $\hat{\phi}_{S,1}$, the direction locally parallel to the MPEP. Similarly, $\lambda_{\perp}(U) = -\partial u_{U,2}/\partial \phi_{U,2}$ is the eigenvalue of the linearized negative drift field at U whose corresponding eigenvector points along $\hat{\phi}_{U,2}$, the direction locally perpendicular to the MPEP, and so forth. $\lambda_{\parallel}(U)$ is the eigenvalue of the linearized negative drift field at U that corresponds to the unstable, or ‘downhill’ direction; it is negative. Eq. (21), which is called the Eyring formula, is a version of the Kramers rate formula that incorporates transverse fluctuations.

In a spatially extended equilibrium system, where the evolution equation is a stochastic *partial* differential equation (cf. (2)), Eq. (21) generalizes in a formally (though not computationally) straightforward way [8]. Because of the field-theoretic nature of the model, the linearized dynamics at each fixed point have a countable infinity of eigenvalues. The generalization of the prefactor Γ_0 of (21) is

$$\Gamma_0 = \frac{|\lambda_0(\phi_u)|}{2\pi} \sqrt{\frac{\prod_{n=0}^{\infty} \lambda_n(\phi_s)}{\prod_{n=0}^{\infty} |\lambda_n(\phi_u)|}}, \quad (22)$$

where ϕ_s is the stable configuration and ϕ_u is the dominant saddle. Here $\lambda_0(\phi_u)$, which is the only negative eigenvalue in the sets $\{\lambda_n(\phi_u)\}_{n=0}^{\infty}$ and $\{\lambda_n(\phi_s)\}_{n=0}^{\infty}$, is the negative eigenvalue of the linearization of the negative drift field $\delta\mathcal{H}/\delta\phi$ at the transition state ϕ_u . It corresponds to the unstable direction. It is easy to see that in the case of a two-dimensional order parameter, in which there are only two eigenvalues at each stationary state, (22) reduces to the Eyring formula (21). $\lambda_{\parallel}(U)$ corresponds to $\lambda_0(\phi_u)$.

Because both the numerator and denominator of the quotient inside the square root are products of an infinite number of eigenvalues (typically with magnitude much greater than unity, as will shortly be seen), they may diverge. However, their *ratio*, defined in a limiting sense, will generally be finite.

It is often not possible to compute in closed form the eigenvalue spectrum of the linearized zero-noise dynamics at the relevant stationary points (although an exception will be seen below). To employ standard techniques for prefactor computation, the above formula may optionally be recast as a *determinant quotient* of the linearized time-evolution operators at the fixed points [1, 8, 21, 24]. Consider a small perturbation η about the stable state, i.e., $\phi = \phi_s + \eta$. Then to leading order $\dot{\eta} = -\hat{\Lambda}[\phi_s]\eta$, where $\hat{\Lambda}[\phi_s]$, which is the Hessian operator $\delta^2\mathcal{H}/\delta\phi^2$ evaluated at $\phi = \phi_s$, specifies the linearized zero-noise dynamics at ϕ_s . Similarly, $\hat{\Lambda}[\phi_u]$ specifies the linearized zero-noise dynamics at ϕ_u . For notational convenience, we shall write λ_n^s and λ_n^u for $\lambda_n(\phi_s)$ and $\lambda_n(\phi_u)$. As above, let λ_0^u be the only negative eigenvalue of $\hat{\Lambda}[\phi_u]$, corresponding to the direction along which the MPEP approaches the transition state. Then

$$\Gamma_0 = \frac{|\lambda_0^u|}{2\pi} \sqrt{\frac{\det \hat{\Lambda}[\phi_s]}{|\det \hat{\Lambda}[\phi_u]|}} \quad (23)$$

is an alternative expression for Γ_0 . The two determinants are typically not defined, but their quotient can be made sense of in any of several ways: as a limit of determinant quotients arising from finite-dimensional truncations, for instance.

In the stochastic Ginzburg–Landau model of (2), it is straightforward to compute the differential operators $\hat{\Lambda}[\phi_s]$ and $\hat{\Lambda}[\phi_u]$. Linearizing the zero-noise evolution $\dot{\phi} = -\delta\mathcal{H}/\delta\phi$ at any stationary state $\phi = \phi_0$ yields

$$\dot{\eta} = -\hat{\Lambda}[\phi_0] \eta \equiv -\left[-d^2/dx^2 + (-1 + 3\phi_0^2)\right] \eta. \quad (24)$$

With the formulas (23) and (24) in hand, we shall now work out the Kramers rate prefactor in the Neumann case, as a illustrative calculation.

5.1 The Neumann-Case Rate Prefactor When $L < L_c$

If $L < L_c^N = \pi$, both the stable and transition states are spatially uniform: $\phi_s \equiv \pm 1$ and $\phi_u \equiv 0$. This greatly simplifies the computation of the associated eigenvalues. Note that the eigenvalue spectrum is the same at both stable states, by symmetry under $\phi \mapsto -\phi$; and because only the square ϕ_0^2 appears on the right-hand side of (24).

Linearizing around either stable state yields the operator

$$\hat{\Lambda}[\phi_s] = -d^2/dx^2 + 2, \quad (25)$$

and similarly

$$\hat{\Lambda}[\phi_u] = -d^2/dx^2 - 1. \quad (26)$$

The eigenvalue spectrum of $\hat{\Lambda}[\phi_s]$, equipped with Neumann boundary conditions, is

$$\lambda_n^s = 2 + \frac{\pi^2 n^2}{L^2}, \quad n = 0, 1, 2, \dots \quad (27)$$

The eigenvalue spectrum of $\hat{\Lambda}[\phi_u]$ is similarly

$$\lambda_n^u = -1 + \frac{\pi^2 n^2}{L^2}, \quad n = 0, 1, 2, \dots \quad (28)$$

As expected, all eigenvalues of $\hat{\Lambda}[\phi_s]$ are positive, while the $\hat{\Lambda}[\phi_u]$ operator has a single negative eigenvalue (with value -1). The corresponding eigenfunction, which is spatially uniform, is the direction in configuration space along which the MPEP approaches ϕ_u .

Putting everything together, we find the Neumann-case rate prefactor when $L < L_c^N = \pi$ to be

$$\begin{aligned} \Gamma_0 &= \frac{1}{2\pi} \sqrt{\frac{\prod_{n=0}^{\infty} (2 + \frac{\pi^2 n^2}{L^2})}{|\prod_{n=0}^{\infty} (-1 + \frac{\pi^2 n^2}{L^2})|}} \\ &= \frac{1}{2^{3/4}\pi} \sqrt{\frac{\sinh(\sqrt{2}L)}{\sin L}}, \end{aligned} \quad (29)$$

where the latter expression follows from the well-known infinite product representation for the sine. This diverges as $L \rightarrow \pi^-$, i.e., as $L \rightarrow (L_c^N)^-$. In this limit, $\Gamma_0 \sim \text{const} \times (L_c^N - L)^{-1/2}$. As mentioned in the introduction, this divergence has a simple physical interpretation: it arises from the MPEP becoming *transversally unstable* as $L \rightarrow (L_c^N)^-$. In the endpoint linearization framework, the divergence is caused by the eigenvalue λ_1^u tending to zero. The appearance of a zero eigenvalue signals the appearance of a transverse soft mode.

5.2 The Neumann-Case Rate Prefactor When $L > L_c$

When $L > L_c^N$, there are two transition states: the nonuniform droplet pair configurations $\pm\phi_u$, one of which is shown in Fig. 2. Closed-form computation of the eigenvalues of the linearized

dynamics at a nonuniform stationary state is generally not possible. However, there are well-known techniques for computing the determinant quotient in (23). The transition state ϕ_u is given by (13), with $m = m(L)$ (for ease of notation, all subscripts will be dropped) determined implicitly by (14). The associated linearized evolution operator, computed from (24), is

$$\hat{\Lambda}[\phi_u] = -\frac{d^2}{dx^2} - 1 + \frac{6m}{m+1} \operatorname{sn}^2 \left(\frac{x}{\sqrt{m+1}} + \mathbf{K}(m) \mid m \right). \quad (30)$$

Evaluation of Γ_0 requires the calculation of the eigenvalue spectrum of this unusual Schrödinger operator, or at least the calculation of an associated determinant quotient. It is worth mentioning that a similar Schrödinger operator arises in the analyses of Langer and Callan–Coleman. However, since they considered only the limit $L \rightarrow \infty$, which corresponds to $m \rightarrow 1^-$, the ‘potential energy’ in their Schrödinger operators involves hyperbolic trigonometric functions rather than elliptic functions. For a careful review, see Ref. [21].

Calculation of the associated determinant quotient is facilitated by the following fact, which was first noticed by Gel’fand (c. 1960). Let $\eta_{u,*}$ be a nonzero solution on $[0, L]$ of the homogeneous equation

$$\hat{\Lambda}[\phi_u]\eta = 0, \quad (31)$$

and let $\eta_{s,*}$ be chosen similarly. Then if $\eta_{u,*}, \eta_{s,*}$ satisfy a Neumann boundary condition at $x = 0$, i.e.,

$$\eta'_{u,*}|_0 = \eta'_{s,*}|_0 = 0, \quad (32)$$

it can be shown that [25, 12]

$$\frac{\det \hat{\Lambda}[\phi_s]}{\det \hat{\Lambda}[\phi_u]} = \frac{\eta'_{s,*}|_L \eta_{u,*}|_0}{\eta'_{u,*}|_L \eta_{s,*}|_0}. \quad (33)$$

This reduces the calculation to a series of manipulations of solutions of homogeneous Schrödinger equations.

Consider first the ratio $\eta'_{u,*}|_L / \eta_{u,*}|_0$. A solution of the homogeneous equation (31) that satisfies the Neumann boundary conditions can be found (see Ref. [12]) by differentiating the periodic instanton solution (13) with respect to m ; the result is

$$\begin{aligned} \eta_{u,*}(z; m) = & \frac{1+m^2}{(1-m)\sqrt{2m(1+m)^3}} \operatorname{sn}(z|m) - \sqrt{\frac{m}{2(1+m)}} \frac{1}{1-m} \operatorname{sn}^3(z|m) \\ & + \frac{1}{\sqrt{2m(1+m)^3}} \operatorname{cn}(z|m) \operatorname{dn}(z|m) \left[z - \mathbf{K}(m) + \frac{1+m}{1-m} (\mathbf{E}(m) - \mathbf{E}(z|m)) \right], \end{aligned} \quad (34)$$

where $z \equiv x/\sqrt{m+1} + \mathbf{K}(m)$, and $\operatorname{cn}(\cdot | m)$ and $\operatorname{dn}(\cdot | m)$ are Jacobi elliptic functions [20]. This yields

$$\eta'_{u,*}|_L / \eta_{u,*}|_0 = 2[(1-m)\mathbf{K}(m) - (1+m)\mathbf{E}(m)]. \quad (35)$$

The other ratio in (33) is easily computed by choosing $\eta_{s,*} = \cosh(\sqrt{2}x)$, which yields

$$\eta'_{s,*}|_L / \eta_{s,*}|_0 = \sqrt{2} \sinh(\sqrt{2}L). \quad (36)$$

This is consistent with the numerator of (29), which was obtained through direct computation of the eigenvalue spectrum. Substituting (35) and (36) into (33) yields a formula for the determinant quotient.

Finally, we compute the single negative eigenvalue λ_0^u of $\hat{\Lambda}[\phi_u]$, which is associated with downhill motion away from the transition state ϕ_u . It is easy to check that the corresponding eigenfunction is

$$\eta_{u,0}(x; m) = \text{sn}^2 \left(\frac{x}{\sqrt{m+1}} + \mathbf{K}(m) \mid m \right) - \frac{1}{1+m-\sqrt{m^2-m+1}}. \quad (37)$$

In physical terms, this eigenfunction specifies the way in which a droplet pair configuration in the Neumann model begins to collapse, due to the boundary between the positive and negative droplets, which is a kink initially localized at $x = L/2$ (see Fig. 2) tending to move toward $x = 0$ or $x = L$, where it will be annihilated. The negative eigenvalue itself is

$$\lambda_0^u = 1 - \frac{2}{1+m} \sqrt{m^2 - m + 1}, \quad (38)$$

which approaches -1 as $m \rightarrow 0^+$, i.e., as $L \rightarrow (L_c^N)^+$, in agreement with the single negative eigenvalue of (28). As $m \rightarrow 1^-$ (i.e., as $L \rightarrow \infty$), $\lambda_0^u \rightarrow 0$ as $\text{const} \times \exp(-L\sqrt{2})$. This implies that the zero-noise motion of the kink domain wall between the positive and negative droplets, which, since it leads to annihilation of the kink, is a deterministic ‘coarsening’ phenomenon (cf. Ref. [26]), proceeds only very slowly in the limit of large L . In the same limit, the numerator of the determinant quotient diverges only as $\exp(L/\sqrt{2})$, so the Kramers rate prefactor tends to zero.

As an interesting aside, we note that the eigenvalue equation for the operator $\hat{\Lambda}[\phi_u]$ of (30) is the spin-2 Lamé equation [27], which is a Schrödinger equation with an elliptic potential. This potential is periodic, with lattice constant $2\mathbf{K}(m)$. So the spectrum of $\hat{\Lambda}[\phi_u]$ has a band structure. This observation facilitates the calculation of the eigenvalues of $\hat{\Lambda}[\phi_u]$, which can be viewed as band edges; and, though we do not supply details here, the calculation of associated determinant quotients. The fact that the Lamé equation is the eigenvalue equation that governs the stability of periodic instanton configurations has previously been noticed by others [28, 29], though mostly in a quantum context.

Putting everything together, we find the Neumann-case rate prefactor when $L > L_c^N = \pi$ to be

$$\Gamma_0 = \frac{1}{\pi} \left| 1 - \frac{2}{1+m} \sqrt{m^2 - m + 1} \right| \sqrt{\frac{\sinh(\sqrt{2}L)}{\sqrt{2} |(1-m)\mathbf{K}(m) - (1+m)\mathbf{E}(m)|}}. \quad (39)$$

Compared to the formula (23) for Γ_0 , this includes an extra factor of 2, since there are two transition states: ϕ_u and $-\phi_u$. As $m \rightarrow 0$ (i.e., as $L \rightarrow (L_c^N)^+$), Γ_0 diverges as $\text{const} \times (L - L_c^N)^{-1/2}$. It should be noted that as $L \rightarrow (L_c^N)^+$ and $L \rightarrow (L_c^N)^-$, the prefactor diverges according to the same inverse power law.

The divergence at $L = \pi$ is certainly striking, and leads one to wonder how, when $L = \pi$ exactly, the Kramers rate formula $\Gamma \sim \Gamma_0 \exp(-\Delta W/\epsilon)$ should be modified. Presumably, it should be replaced by

$$\Gamma \sim \text{const} \times \epsilon^{-\alpha} \exp(-\Delta W/\epsilon), \quad \epsilon \rightarrow 0, \quad (40)$$

for some $\alpha > 0$. The computation of the exponent α and the factor ‘const’, and of course the divergence of the rate prefactor at $L = L_c$ for the other choices of boundary condition, will be considered elsewhere.

Acknowledgments

This research was supported in part by National Science Foundation Grant No. PHY-0099484.

References

- [1] F. Moss and P. V. E. McClintock, eds., *Theory of Continuous Fokker–Planck Systems*, vol. 1 of *Noise in Nonlinear Dynamical Systems*, Cambridge University Press, Cambridge, UK, 1989.
- [2] M. C. Cross and P. C. Hohenberg, “Pattern formation outside of equilibrium,” *Rev. Modern Phys.* **65**, pp. 851–1111, 1993.
- [3] U. Bisang and G. Ahlers, “Thermal fluctuations, subcritical bifurcation, and nucleation of localized states in electroconvection,” *Phys. Rev. Lett.* **80**(14), pp. 3061–3064, 1998.
- [4] H.-B. Braun, “Thermally activated magnetization reversal in elongated ferromagnetic particles,” *Phys. Rev. Lett.* **71**(21), pp. 3557–3560, 1993.
- [5] G. Brown, M. A. Novotny, and P. A. Rikvold, “Micromagnetic simulations of thermally activated magnetization reversal of nanoscale magnets,” *J. Appl. Phys.* **87**(9), pp. 4792–4794, 2000. Available as arXiv: cond-mat/9909136.
- [6] G. Blatter, M. V. Feigel’man, V. B. Geshkenbein, A. I. Larkin, and V. M. Vinokur, “Vortices in high-temperature superconductors,” *Rev. Modern Phys.* **66**, pp. 1125–1388, 1994.
- [7] J. Buerki, C. Stafford, and D. L. Stein, “Thermal instabilities of alkali and noble metal nanowires.” In preparation, 2003.
- [8] J. S. Langer, “Statistical theory of the decay of metastable states,” *Ann. Physics* **54**, pp. 258–275, 1969.
- [9] C. Callan and S. Coleman, “Fate of the false vacuum, II. First quantum corrections,” *Phys. Rev. D* **16**, pp. 1762–1768, 1977.
- [10] W. G. Faris and G. Jona-Lasinio, “Large fluctuations of a nonlinear heat equation with noise,” *J. Phys. A* **15**(10), pp. 3025–3055, 1982.
- [11] F. Martinelli, E. Olivieri, and E. Scoppola, “Small random perturbations of finite and infinite dimensional dynamical systems: Unpredictability of exit times,” *J. Statist. Phys.* **55**(3/4), pp. 477–504, 1989.
- [12] A. J. McKane and M. B. Tarlie, “Regularization of functional determinants using boundary conditions,” *J. Phys. A* **28**(23), pp. 6931–6942, 1995. Available as arXiv: cond-mat/9509126.
- [13] R. S. Maier and D. L. Stein, “Droplet nucleation and domain wall motion in a bounded interval,” *Phys. Rev. Lett.* **87**(27), pp. 270601–1–270601–4, 2001. Available as arXiv: cond-mat/0108217.

- [14] E. M. Chudnovsky, “Phase transitions in the problem of the decay of a metastable state,” *Phys. Rev. A* **46**(12), pp. 8011–8014, 1992.
- [15] A. N. Kuznetsov and P. G. Tinyakov, “Periodic instanton bifurcations and thermal transition rate,” *Phys. Lett. B* **406**(1–2), pp. 76–82, 1997. Available as arXiv: hep-ph/9704242.
- [16] D. L. Stein, “Critical behavior of the Kramers escape rate in asymmetric classical field theories.” Submitted to *J. Stat. Phys.*, 2003.
- [17] H.-B. Braun, “Nucleation in ferromagnetic nanowires — magnetostatics and topology,” *J. Appl. Phys.* **85**(8), pp. 6172–6174, 1999.
- [18] R. Rajaraman, *Solitons and Instantons: An Introduction to Solitons and Instantons in Quantum Field Theory*, North-Holland, New York/Amsterdam, 1982.
- [19] J. A. Espichán Carrillo, A. Maia, Jr., and V. M. Mostepanenko, “Jacobi elliptic solutions of $\lambda\phi^4$ theory in a finite domain,” *Int. J. Mod. Phys. A* **15**(17), pp. 2645–2659, 2000. Available as arXiv: hep-th/9905151.
- [20] M. Abramowitz and I. A. Stegun, eds., *Handbook of Mathematical Functions*, Dover, New York, 1965.
- [21] L. S. Schulman, *Techniques and Applications of Path Integration*, Wiley, New York, 1981.
- [22] R. S. Maier and D. L. Stein, “Theory of the condensation point in systems of finite extent.” In preparation, 2003.
- [23] C. W. Gardiner, *Handbook of Stochastic Models*, Springer-Verlag, New York/Berlin, second ed., 1985.
- [24] P. Hänggi, P. Talkner, and M. Borkovec, “Reaction-rate theory: Fifty years after Kramers,” *Rev. Modern Phys.* **62**(2), pp. 251–341, 1990.
- [25] R. Forman, “Functional determinants and geometry,” *Invent. Math.* **88**(3), pp. 447–493, 1987. Erratum in **108**(2), pp. 453–454, 1992.
- [26] S. Habib and G. Lythe, “Dynamics of kinks: Nucleation, diffusion, and annihilation,” *Phys. Rev. Lett.* **84**(6), pp. 1070–1073, 2000. Available as arXiv: cond-mat/9911228.
- [27] H. Li, D. Kusnezov, and F. Iachello, “Group-theoretical properties and band structure of the Lamé Hamiltonian,” *J. Phys. A* **33**(36), pp. 6413–6429, 2000.
- [28] J.-Q. Liang, H. J. W. Müller-Kirsten, and D. H. Tchrakian, “Solitons, bounces and sphalerons on a circle,” *Phys. Lett. B* **282**(1–2), pp. 105–110, 1992.
- [29] J.-G. Caputo, N. Flytzanis, Y. Gaididei, N. Stefanakis, and E. Vavalis, “Stability analysis of static solutions in a Josephson junction,” *Supercond. Sci. Technol.* **13**, pp. 423–438, 2000. Available as arXiv: cond-mat/0010335.